# Part-load Performance of Direct-firing and Co-firing of Coal and Biomass in a Power Generation System Integrated with a $CO_2$ Capture and Compression System

Usman Ali[a, c,*], Muhammad Akram[a], Carolina Font-Palma[b], Derek B Ingham[a], Mohamed Pourkashanian[a]

[a]*Energy 2050, Energy Engineering Group, Faculty of Engineering, University of Sheffield, Faculty of Engineering, S10 2TN, UK*

[b]*Department of Chemical Engineering, Thornton Science Park, University of Chester, CH2 4NU, UK*

[c]*Department of Chemical Engineering, University of Engineering and Technology, Lahore – 54890, Pakistan*

## Abstract:

Bioenergy with Carbon Capture and Storage (BECCS) is recognised as a key technology to mitigate $CO_2$ emissions and achieve stringent climate targets due to its potential for negative emissions. However, the cost for its deployment is expected to be higher than for fossil-based power plants with CCS. To help in the transition to fully replace fossil fuels, co-firing of coal and biomass provide a less expensive means. Therefore, this work examines the co-firing at various levels in a pulverised supercritical power plant with post-combustion $CO_2$ capture, using a fully integrated model developed in Aspen Plus. Co-firing offers flexibility in terms of the biomass resources needed. This work also investigates flexibility within operation. As a result, the performance of the power plant at various part-loads (40%, 60% and 80%) is studied and compared to the baseline at 100%, using a constant fuel flowrate. It was found that the net power output and net efficiency decrease when the biomass fraction increases for constant heat input and constant fuel flow rate cases. At constant heat input, more fuel is required as the biomass fraction is increased; whilst at constant fuel input, derating occurs, e.g. 30% derating

* Corresponding Author: chemaliusman@gmail.com

of the power output capacity at firing 100% biomass compared to 100% coal. Co-firing of coal and biomass resulted in substantial power derating at each part-load operation.

*Key words*: Co-firing; post-combustion; part-load; $CO_2$ compression; BECCS

## 1. Introduction

Biomass is becoming increasingly more important for achieving EU emission reduction targets as a renewable energy source (Bertrand et al., 2014). In the UK, bioenergy is mostly used to provide heat or power, where 5.2 GW of bio-power and 3.1 GW of heat were produced at the end of July 2016 (BEIS, 2016). A recent report on trends and projections towards Europe's climate and energy targets for 2020 has shown that in 2013 the European greenhouse gas (GHG) emissions were 19 % lower than the 1990 levels and expected to be 24 % lower by 2020 (Barbu et al., 2014). However, a later report suggested that the pace of GHG reductions will slow down, and by 2030 the EU emissions reduction will be 27-30 % lower than the 1990 levels rather than the target value of 40 % (Barbu et al., 2015). In order to meet the target, there may be an increase in the use of biomass for heat and power to increase the renewable's share of the total energy produced. It is predicted that biomass exploitation capacity in the EU will increase to 1.5-1.8 billion tons in 2030 (EU Commission, 2006).

Biomass in combination with coal, termed as co-firing, represents one possible option for reducing $CO_2$ emissions (Heller et al., 2004; Jia et al., 2016; Mann and Spath, 2001; Ortiz et al., 2011; Rigamonti et al., 2012; Sebastián et al., 2011) and can add flexibility to the system.

In addition to reducing GHG emissions, co-firing has added advantages. Co-firing can result in the reduction of $NO_x$ and $SO_x$ emissions, depending upon the type of fuel and operational conditions (De and Assadi, 2009). Furthermore, co-firing can result in the reduction in corrosion, fouling and slagging problems caused by firing biomass alone (Davidsson et al., 2008; NETBIOCOF, 2016; Tillman, 2000). However, a drop-in efficiency of the boiler can be expected due to co-firing which is modest at lower co-firing ratios (De and Assadi, 2009; Hughes and Tillman, 1998; NETBIOCOF, 2016).

During co-firing, biomass and coal result in synergistic interaction due to the presence of volatiles in biomass (Oladejo et al., 2017; Sung et al., 2016; Tilghman and Mitchell, 2015). There is a dominant synergistic impact of co-firing woody biomass with coal under air staged conditions on the emissions of $NO_x$ due to lower carbon content but higher volatile matter in biomass (Sung et al., 2016). Tilghman and Mitchell, (2015) developed an intrinsic chemical reactivity model to predict char conversion rates by using the mass lost data during combustion and gasification. The heterogeneous reaction mechanism model is used to accurately predict the effects of heterogeneous reactions in combustion, gasification and oxy-fuel environments (Tilghman and Mitchell, 2015). Oladejo et al. (2017) developed an index to quantify the degree of synergistic interactions which can be used to select the proper biomass and blending ratio at co-fired power plants.

Co-firing biomass has also been found to be beneficial during the gasification process. During steam co-gasification of 50:50 wt. % coal:switchgrass mixtures in a pilot-scale bubbling fluidized bed, Masnadi et al. (2015c) observed higher hydrogen and cold gas efficiencies, gas yields and HHV of the product gas as compared to single fuel gasification (Masnadi et al., 2015c). The significant enhancement in the production of hydrogen during in-situ capture of $CO_2$ by CaO sorbent has been observed (Masnadi et al., 2015a).

Different behaviours in the reactivity of chars produced from coal and biomass, both together and separately (Ellis et al., 2015). Ellis et al. (2015) suggested that there is an interaction during volatilisation that effects the reactivity and that is why specific and intrinsic rates were observed to be lower when coal and biomass were pyrolyzed together. Potassium in biomass, as excess potassium (K/Al >1), can result in enhanced coal gasification due to its catalytic impact (Habibi et al., 2012). The catalytic impact of potassium in biomass when the biomass to coal ratio reached 3:1, where the biomass supplied enough potassium to satisfy the minerals in the coal ash to enhance coal gasification has been found in the literature (Masnadi et al., 2015b).

Co-firing is a proven technology with a significant experience in Europe (Al-Mansour and Zuwala, 2010). The share of biomass co-firing in conventional pulverised coal fired power stations have increased by up to 20 % in the past decade with some installations demonstrating a complete switch from coal to biomass (Cremers, 2009).

Biomass and coal have different burnout rates and therefore may be fed to the combustor at different locations (Jia et al., 2016). Also, coal and biomass can be mixed before combustion to achieve a better control of the combustion process (Sahu et al., 2014). In the co-firing process, biomass is mixed with coal to achieve over 35 % volatile matter for a stable flame (Biagini et al., 2002; Wang et al., 2009). In the UK, co-firing biomass with coal offers a better opportunity as compared to a dedicated biomass plant due to relatively small bioenergy resources (Gough and Upham, 2011). In addition, biomass power is produced in either old coal power plants converted to operate on imported biomass, e.g. Drax 2 and Ironbridge 1 and 2 (Verhoest and Ryckmans, June 2014), or purpose built biomass power plants, e.g. Stevens Croft (40MW) that uses sawmill waste (AG., 2014).

In modern coal fired power plants, biomass can be co-fired up to 15 % without steam boiler modifications and existing environmental control systems can be used at higher biomass co-firing rates with minor modification (IEA, January 2007). Moreover, co-firing gives substantially higher net efficiency than that a dedicated biomass fired power plant can deliver (Hetland et al., 2016). This makes co-firing a much less expensive option than building a dedicated biomass power plant (IEA, January 2007). In the absence of financial incentives for negative emissions and avoided carbon, co-firing can play a transitional role to minimise the emission penalties in a cost effective way (ETI, 2016). Moreover, the plant can be adjusted to perform optimally using different types of biomass (Hetland et al., 2016). If the biomass supply is ceased, due to a short age of supply, natural calamities or logistic issues, coal is still available to keep the lights on and life moving. Biomass combustion can generate various types of pollutants depending upon the type of combustion technology employed, properties of the biomass used and pollutant control measures adopted can be found in the literature (Loo and Koppejan, 2002). Also co-firing contributes to the reduction in emissions of obnoxious gases, such as $SO_x$ and $NO_x$.

Immediate step changes in emissions reduction is required to control $CO_2$ concentration in the atmosphere. If drastic measures are not adapted, then by the end of the century $CO_2$ concentration in the atmosphere could reach 650 ppmv, or even higher (Anderson and Bows, 2008). Reduction in GHG emissions can improve air quality (Driscoll et al., 2015; Thompson et al., 2014; West et al., 2013) and also limit global warming. There are many GHG emissions reduction options, such as energy savings and renewable energy technologies, but CCS, amongst others, is considered to be a key technology to meet stringent climate targets (Koornneef et al., 2012). CCS comprises three steps; capture from the point source, transport and storage. Although the individual technologies have been demonstrated with much operational experience and are relatively well understood, however, the deployment of a large scale fully integrated commercial CCS process is a key challenge (Gough and Upham, 2011).

Most of the biomass power plants deployed are fairly small units (1-100$MW_e$) and this is due to the limited local feedstock availability and high transportation costs (IEA, January 2007). Due to this reason, costs associated with bioenergy with Carbon Capture and Storage (BECCS) are likely to be higher as compared to those associated with fossil fuel fired power plants with

CCS (Azar et al., 2006). However, in the UK the Drax power plant has 4 GW total capacity with 70 % biomass share, and it is big enough to deliver economies on a scale for capturing $CO_2$ (ETI, 2016). Moreover, there is sufficient potential for bioenergy to make a significant contribution to the global energy supply (Dornburg et al., 2010).

In order to meet the target of limiting the global warming to below 2 °C, more than 1 Gt/year of negative emissions are required (Gasser et al., 2015) and BECCS significantly enhances the chances of meeting these ambitious climate mitigation targets (Azar et al., 2010). Each unit of energy produced from BECCS is twice as effective in mitigating emissions as the ones without CCS (Muratori et al., 2016). BECCS may be referred to as the process of capturing $CO_2$ emissions from biomass fired power plants and storing $CO_2$ in geological formations, or using as a feedstock to produce algal biomass which is then converted to transport fuel, animal feed or plastics (Gough and Upham, 2011). BECCS can be used to produce electricity, heat, gaseous and liquid fuels and result in net removal of $CO_2$ from the atmosphere, also termed as "negative emission" (ETI, 2016). BECCS potentially could have 33 % share of overall emissions mitigation by the end of the century (Klein et al., 2011). According to the Fifth Assessment Report of the Intergovernmental Panel on Climate Change (IPCC) it will not be possible to achieve the target of limiting global warming without the wide spread deployment of Bio-Energy, CCS and their combination (IPCC, 2014). BECCS can reduce the cost of achieving the climate target by offsetting $CO_2$ from other sectors such as transportation, which are more expensive to decarbonise (Luckow et al., 2010).

BEECS is a natural technology to progress first as it is competitive with other clean technologies, adds flexibility to the system, has capacity to deliver negative emissions and reduces the overall cost of decarbonisation (Oxburgh, 2016). According to a recent report published by the Energy Technologies Institute (ETI), about half of the UK's 2050 emissions reduction target (c.55 million tonnes of negative annual emissions) could be delivered by deploying BECCS and could reduce the cost of meeting GHG emissions targets of the UK by up to 1 % of GDP and that BECCS is one of the few practical, scalable and economic technologies having UK relevance for removing $CO_2$ from the atmosphere in large quantities (ETI, 2016).

The most significant barrier to the deployment of BECCS is not technical but economic and regulatory (Bhave et al., 2014). In the near future, cost saving will not be delivered through fundamental technology break-through but through reducing costs by deployment (ETI, 2016). According to the Global CCS Institute database, no BECCS demonstration project has, as yet, materialised (GCCSI, 2016). There are some bioethanol production based on BECCS projects currently in operation (GCCSI, 2011) but power based BECCS projects are almost non-existent. The Mikawa biomass power plant (49 MW) with $CO_2$ capture in Japan is aimed at being operational in 2020 and it will be the first power plant in the world that is capable of delivering negative emissions (Toshiba, 2016). The Maasvlakte power plant 3 (MPP3) in the Netherlands has a capacity of 1070 $MW_e$ and it became operational in 2015 being capable of accepting up to 30 % biomass and is CCS ready subject to commercial decision (GCCSI, 2015). According to a recent report by the Global CCS Institute (GCCSI, 2016), the Illinois Industrial CCS project (1 Mtpa $CO_2$ capture capacity) is the world's first large scale industrial BECCS project and is expected to begin operation in early 2017. The technology will move closer to commercialisation as more demonstration projects come online (Gough and Upham, 2011).

In spite of all the benefits of BECCS, the deployment of CCS may be delayed due to the temptation that BECCS can remove the $CO_2$ already emitted to the atmosphere (Muratori et al., 2016) and thus can be deployed at a later date. However, this notion of delaying will lead to catastrophic consequences to the world in terms of environmental as well as economic implications.

### 1.1 Novelty and Contribution

Process modelling is used as an effective mean for better understanding for different operating levels of the power plant with $CO_2$ capture due to lower cost in comparison to pilot-scale and demonstration studies. The base load performance of the power plant for fossil fuels is successfully investigated through process modelling and simulation. The reporting of part-load analysis of the power plant for fossil fuels with $CO_2$ capture is limited and few studies can be found in the literature (Adams and Mac Dowell, 2016; Alobaid et al., 2014; Biliyok et al., 2012; Fernandez et al., 2016; Hanak et al., 2015; Jordal et al., 2012; Möller et al., 2007; Nord et al., 2009). However, most of the studies report the part-load performance and operational flexibility of a standalone natural gas power plant (Alobaid et al., 2014) or their integration with the amine-based $CO_2$ capture plant for interim operation and/or by-pass of the $CO_2$ capture plant (Adams and Mac Dowell, 2016; Jordal et al., 2012; Möller et al., 2007; Nord et al., 2009). The part-load operation of the coal-fired power plant integrated with an amine-based $CO_2$ capture plant has been reported in the literature (Fernandez et al., 2016; Hanak et al., 2015). Fernandez et al. (2016) have discussed the operational flexibility of the coal-fired power plant, with interim solvent regeneration and $CO_2$ capture plant by-pass at peak-load demand, however, it lacks the comprehensive details of the process and its parameters. Hanak et al. (2015) have reported the thorough details of the whole process of the coal-fired power plant integrated with $CO_2$ capture plant, at base-load and part-load performance. However, none have taken the biomass into consideration either at base-load or at part-load operation, neither as direct-firing nor as co-firing of coal with biomass.

The above discussion has shown that BECCS is a key technology to meet GHG emissions reduction targets and that co-firing biomass in coal fired systems has several advantages over dedicated biomass firing systems. Only a few studies have investigated BECCS for the commercial-scale application, as reported in the literature (Ali et al., 2017; Berstad et al., 2011;

Hetland et al., 2016). Berstad et al. (2011) have compared the three different power plants integrated with MEA-based $CO_2$ capture plant including, natural gas, coal and biomass at varying stripper pressure. Berstad et al. (2011) have found that the coal and biomass power plants with a MEA-based $CO_2$ capture plant results in lower specific losses per unit of the $CO_2$ captured. However, this study was limited to the assessment of the base-load performance of varying nominal power output for natural gas, coal and biomass -fired power plants with limited details. Hetland et al. (2016) presented direct-firing and co-firing cases of coal and biomass, however, only one case of co-firing is presented in detail with no attempt for the part-load operation. Furthermore, the detailed information and parameters about the power plant and CCS is lacking. Ali et al. (2017) have assessed the comparative potential of natural gas, coal and biomass for the supercritical power plant integrated with $CO_2$ capture plant and $CO_2$ compression system. However, it does not take into account the co-firing and part-load operation.

Due to limited information found in the open literature, it is important to assess the performance of the part-load performance of direct-firing and co-firing of coal and biomass, especially integrated with a $CO_2$ capture plant and $CO_2$ compression unit. Neither the integration of direct-firing and co-firing with a $CO_2$ capture plant and $CO_2$ compression unit at the base-load has been extensively studied before nor the part-load performance of the integration of direct-firing and co-firing with $CO_2$ capture plant and $CO_2$ compression unit. Therefore, this paper presents a detailed investigation of the co-firing of coal and biomass for commercial-scale pulverised supercritical power plants. Further, the integration of the post-combustion $CO_2$ capture plant (CCP) and $CO_2$ compression unit (CCU) is also investigated. Two co-firing scenarios of coal and biomass are investigated at base-load operation of the power plants, i.e. constant heat input (CHI) and constant fuel input (CFF), and the details of which are described in the respective sections. Furthermore, the part-load operation (80, 60 and 40 %) is analysed for co-firing of coal and biomass and integrated with CCP and CCU. Therefore, the theme of the present study is to analyse the base-load performance of the direct-fired and co-fired coal and biomass power plants integrated with CCP and CCU for the CHI and CFF cases. Furthermore, extending the scope of the study towards the part-load operation at different power ratings for both direct-fired and co-fired coal and biomass power plants integrated with CCP and CCU for CFF case.

The whole investigation is realised by the process modelling and simulation tool, Aspen Plus. The solvent employed is monoethanolamine (MEA) of 30 wt. % strength with 90 % of the $CO_2$ capture efficiency. This paper is structured as follows. In Section 2, the process description, along with the modelling strategy, is described in detail. This is followed by the base-load and part-load modelling framework. In Section 3, the results and discussions for the base-load and part-load operation for the co-firing of coal and biomass is presented. Further, the effect of the part-load on the operation of the CCP is also discussed. Finally, conclusions are drawn in Section 4.

232

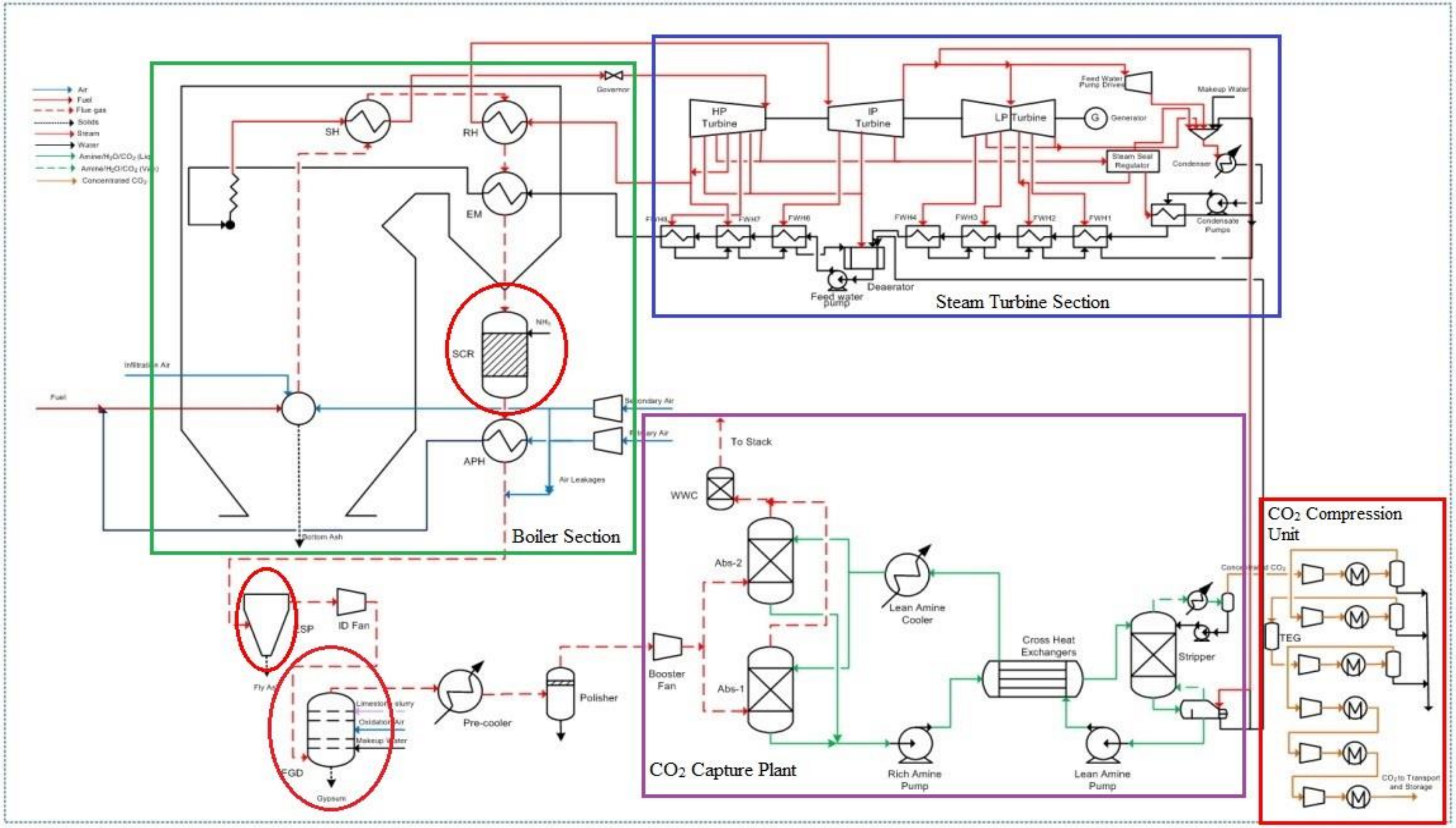


233

234 Figure 1 Process schematic of pulverised solid fuel power plant integrated with MEA-based $CO_2$ capture plant and $CO_2$ compression unit (Ali et al., 2017).

## 2. Process Description

The gross power output of the power plant is 800 $MW_e$ based on the pulverised coal-fired supercritical power plant in the 2010 Report of the Department of Energy (Black, 2010). A schematic of the power plant model developed is shown in Figure 1. The steam generator for the supercritical-type boiler is once-through with superheater, reheater, economizer and air preheater. The steam specification for the supercritical steam turbine is 24.1/593/593 MPa/$^{o}$C/$^{o}$C with single reheat. Initially the feedwater is heated by bleeds of LP turbine, through four feedwater heaters, followed by the deaerator, and three feedwater heaters by bleeds of the HP turbine. The condenser operates at a saturation pressure of 7 kPa. Further, the power plant is equipped with flue gas treatment units, including the selective catalytic reduction unit for $NO_x$ removal using ammonia and catalysts; fabric filters for the particulates removal; the flue gas desulphurization unit for the removal of the $SO_2$ using the wet limestone forced oxidation process; and the $CO_2$ capture plant for the removal of the $CO_2$ using MEA-based reactive absorption and desorption. More details of the flue gas treatment can be found in Ali et al. (2017).

The $CO_2$ capture plant (CCP) is based on post-combustion $CO_2$ capture technology using reactive absorption and desorption. The $CO_2$ capture plant consists of two absorbers and one stripper. The $CO_2$ released from the stripper is compressed to a final pressure of 153 bar using a six-stage $CO_2$ compression unit (CCU) equipped with intercoolers and knock-out drums. The tri ethylene glycol unit is used at the third stage to maintain the $H_2O$ specification of the dense phase $CO_2$ stream.

The air after the split is blown through primary and secondary fans, where the primary fan after air preheating is used to carry the fuel to the boiler, and the secondary air is fed at the latter stage of the boiler. Tertiary air and air leakages are also indicated in the boiler section which is indicated by a green rectangle in Figure 1. The flue gas after combustion of the fuel, either coal, biomass or co-firing of coal and biomass, is used for steam generation in the superheater, reheater and economiser after which the flue gas is cleaned of the $NO_x$ emissions through the SCR as indicated by the red circle in the boiler section of Figure 1. The flue gas is then used to preheat the incoming air from the primary blowers and then the flue gas is cleaned from particulate matter in the ESP, before injecting it to the FGD for $SO_2$ removal which is indicated by the red circles in Figure 1. After that the flue gas is either vented to the chimney or sent to the CCP and CCU sections for the $CO_2$ removal and compression.

The boiler feed water after preheating through the feedwater heaters and treatment through the feedwater deaerating is saturated in the economiser. The saturated steam is then superheated in the superheater. The superheated steam from the superheater is sent to the HP turbine for power generation, the steam after the HP turbine is passed through the reheater and is boosted and passed through the IP turbine. The steam after the pressure reduction in the IP turbine is sent to the LP turbine and a portion to the reboiler of the CCP section. The leakages from slip streams in each section of the turbines are used to preheat the boiler feedwater in the steam turbine section as shown by the blue rectangle in Figure 1.

The CCP section indicated by the purple rectangle in Figure 1 consists of two absorbers and one stripper. The flue gas after the pressure increase in the blower is split into two parts for each absorber. The flue gas after stripping the $CO_2$ from the flue gas using 30 wt. % MEA solution is vented to the chimney. The rich solvent with higher concentration of the $CO_2$ is pumped and heated through the cross-heat exchanger and then fed to the top of the stripper for the regeneration of the solvent through the steam extracted from the IP-LP cross over section of the steam turbine section. The solvent after regeneration is pumped, cooled and fed to the top of the absorber. The $CO_2$ from the CCP is compressed through six stages of the compressors with inter-stage coolers to reach the final pressure of 153 bar. The CCU section is shown by the red rectangle in Figure 1.

The proximate and ultimate analysis of the coal and biomass is shown in Table 1. The coal selected is from the 2010 Report of U.S. Department of Energy (Black, 2010), to have a fair comparison and verification of the results. In spite of the interest in carbon capture and storage, there is less freely available data in the open literature with complete information to rigorously model and validate the supercritical coal-fired power plant except the data reported by Black (2010). Therefore, the composition of coal is fixed to be the same as that found in (Black, 2010) for a fair comparison. The biomass selected in Table 1 is the U.S. forestry residue pellets. Further, the biomass is selected as it will be a basis for future research and experimentation by the UK Carbon Capture and Research Centre's (UKCCSRC) at the Pilot-Scale Advanced $CO_2$ Capture Technology (PACT) National Core Facilities. The experimental data obtained at the PACT facility will be used to validate the models and to perform further assessments. The various case studies performed in this study are case-specific as varying the composition of the coal and biomass are not assessed, however, the conclusions of this study are reasonably general for different co-firing cases covering a wider range of fuel compositions.

Table 1 Proximate, ultimate and heating value of coal (Black, 2010) and biomass (Al-Qayim et al., 2015).

| | Coal | | Biomass Pellets | |
|---|---|---|---|---|
| Proximate Analysis | As-received (wt. %) | Dry (wt. %) | As-received (wt. %) | Dry (wt. %) |
| Moisture | 11.12 | 0.00 | 6.69 | 0.00 |
| Volatile Matter | 34.99 | 39.37 | 78.10 | 83.70 |
| Ash | 9.70 | 10.91 | 0.70 | 0.75 |

| | | | | |
|---|---|---|---|---|
| Fixed Carbon | 44.19 | 49.72 | 14.51 | 15.55 |
| Ultimate Analysis | As-received (wt. %) | Dry (wt. %) | As-received (wt. %) | Dry (wt. %) |
| C | 63.75 | 71.72 | 48.44 | 51.87 |
| S | 2.51 | 2.82 | <0.02 | 0.02 |
| H | 4.50 | 5.06 | 6.34 | 6.79 |
| N | 1.25 | 1.41 | 0.15 | 0.16 |
| O | 6.88 | 7.75 | 37.69 | 40.37 |
| Ash | 9.70 | 10.91 | 0.70 | 0.75 |
| Cl | 0.29 | 0.33 | <0.01 | 0.01 |
| HHV (kJ/kg) | 27113 | 30506 | 19410 | 20802 |
| LHV (kJ/kg) | 26151 | 29444 | 18100 | 19398 |

## 2.1 Modelling Details

As mentioned in Section 1.1, the modelling and simulation of different cases of coal and biomass and their part-load operation is realised in Aspen Plus. The base-case model of super-critical coal-fired power plant is based on the previous work (Ali et al., 2017). The property package employed for the thermodynamic estimation is Peng-Robinson with the Boston-Mathias modification for the boiler, and IAPWS-95 for the steam cycle of the power plant.

The boiler efficiency of 88 % and excess air of 15 % were chosen as recommended in the literature (Stultz and Kitto, 1992). The boiler chemistry is based on the minimization of Gibb's free energy and is used as an equilibrium criterion. It is important to mention here that the non-idealities of the coal and biomass combustion are not taken into consideration. Therefore, the effect of heavy components and tar formation on the combustion kinetics and behaviour for direct-fired and co-fired coal and biomass is outside the scope of the present research. The boiler efficiency and turbine thermal input assists in the estimation of fuel flow rate which further assists in the estimation of air flow rates. The flow rate requirement of ammonia for the SCR unit is estimated from its principal reactions. Similarly, for the FGD unit, the flow rate requirements for lime stone, make-up water and oxygen are estimated based on its principal reactions. The principal reactions for the SCR and FGD units are presented in Table 2. The boiler and steam turbine sections models are validated in the literature (Ali et al., 2017) and verified by the 2010 Report of the Department of Energy (Black, 2010).

Table 2: Principal reactions involved in SCR, FGD and CCP.

| **Reactions** | **Reaction Number** |
|---|---|
| **Selective Catalytic Reduction Unit** | |
| $4NO + 4NH_3 + O_2 \rightarrow 4N_2 + 6H_2O$ + heat | (1) |
| $2NO_2 + 4NH_3 + O_2 \rightarrow 3N_2 + 6H_2O$ + heat | (2) |
| **Flue Gas Desulphurization Unit** | |
| $CaCO_3(s) + SO_2(g) + 0.5H_2O \rightarrow CaSO_3 \cdot 0.5H_2O + CO_2(g)$ | (3) |
| $CaCO_3(s) + SO_2(g) + 0.5O_2 + 2H_2O \rightarrow CaSO_4 \cdot 2H_2O + CO_2(g)$ | (4) |
| **$CO_2$ Capture Plant** | |
| $H_2O + MEAH^+ \leftrightarrow MEA + H_3O^+$ | (5) |
| $2H_2O \leftrightarrow H_3O^+ + OH^-$ | (6) |
| $HCO_3^- + H_2O \leftrightarrow CO_3^{2-} + H_3O^+$ | (7) |
| $CO_2 + OH^- \rightarrow HCO_3^-$ | (8) |
| $HCO_3^- + \rightarrow CO_2 + OH^-$ | (9) |
| $MEA + CO_2 + H_2O \rightarrow MEACOO^- + H_3O^+$ | (10) |
| $MEACOO^- + H_3O^+ \rightarrow MEA + CO_2 + H_2O$ | (11) |

The CCP is modelled using rate-based electrolyte non-random two liquid (ENRTL) thermodynamic packages by incorporating its principal reactions. The design data summary for the CCP is given in Table 4. The aqueous MEA solution with 30 wt. % strength is employed to capture 90 % of the incoming $CO_2$ with 0.2 solvent loading. The CCP model is validated against extensive experimental data in the previous work (Ali et al., 2016). The principal reactions included in the model are mentioned in Table 2. The CCU is modelled with the final pressure of 153 bar. The thermodynamic property package employed for the CCU model is Lee Keser Plocker.

## 2.2 Base-Load Modelling Framework

The reference base-load model for the coal is developed based on the 2010 Report of the Department of Energy (Black, 2010) with a boiler efficiency of 88 %, which assists in the estimation of the fuel flow for 15 % excess air supplied to the boiler. The infiltration air is 2 % of the total air. The different assumptions applied for the modelling of the different sections of the power plant can be found in the quality guidelines provided by the US Department of Energy (Chou et al., 2012, 2014). After analysing the performance of the direct-fired coal-based power plant integrated with CCP and CCU, the co-firing of coal and biomass is performed. The ultimate and proximate analysis of the coal and biomass are shown in Table 1 and it is clear that the biomass will behave differently when fired in the commercial-scale power plant due to the reduced heating value and higher O/C ratio compared to coal. The co-firing of the coal and biomass is incorporated by mixing the biomass with coal, thus defining the common fuel feed composition. The different case studies for the co-firing of coal and biomass are listed in Table 3.

Table 3 Pulverised supercritical co-firing of coal and biomass cases classification* (Ali, 2017).

| Cases | Coal/Biomass percentage in fuel feed stream |
|---|---|
| Coal | 100/0 |
| C8B2 | 80/20 |
| C6B4 | 60/40 |
| C4B6 | 40/60 |
| C2B8 | 20/80 |
| Biomass | 0/100 |

*where ‘C’ represents coal and ‘B’ represents biomass.

Table 4 MEA-based CCP design and operating parameters (Agbonghae et al., 2014).

| Parameter | Value |
|---|---|

| | |
|---|---|
| Absorber | |
| Number of Absorbers | 2 |
| Packing | Mellapak 250Y |
| Packing Height [m] | 23.04 |
| Diameter [m] | 16.13 |
| Stripper | |
| Number of Stripper | 1 |
| Packing | Mellapak 250Y |
| Packing Height [m] | 25.62 |
| Diameter [m] | 14.61 |
| Specific Reboiler Duty [MJ/kg $CO_2$] | 3.69 |
| Flue Gas Flowrate [kg/s] | 821.26 |
| MEA concentration [kg/kg] | 0.3 |
| Lean $CO_2$ loading [mol/mol] | 0.2 |
| Liquid/Gas Ratio [kg/kg] | 2.93 |
| Stripper pressure (Ledda et al.) | 1.62 |

To understand the behaviour of the biomass, two case studies are investigated based on the fuel flowrate. First, the constant heat case (CHI), in which the heat transfer from the boiler to the steam side is kept constant by varying the fuel flowrate while the second one, constant fuel flowrate (CFF) case in which the heat transfer from the boiler to the steam side is varied by keeping the fuel flowrate constant. The base-load performance of the co-firing of coal and biomass is developed for both the CHI and CFF cases integrated with CCP and CCU. A standard MEA-based CCP model, which can service the commercial-scale power plant at 100 % load operation, is developed which can capture 90 % of the $CO_2$ from the flue gas using a 30 wt. % aqueous MEA solution with a lean loading of 0.2. The design and operating parameters of the MEA-based CCP are given in Table 4. The efficiency estimation whether at base-load modelling or part-load modelling is estimated on the basis of the higher heating value. Furthermore, the model predictions of the direct-fired coal-based power plant are in very good agreement with the published data as reported by the author (Ali et al., 2017), and hence the results and findings of the present research may be used with confidence in a ± 10 % margin.

### 2.3 Part-Load Modelling Framework

After developing the base-load performance, the CFF case is evaluated for the part-load performance assessment as it will not result in a major redesign of the boiler section of the power plant. The coal-fired power plant is considered as the basis for each part-load assessment, and then the fuel switch from coal to biomass and co-firing of coal and biomass are evaluated at each part-load operation. The part-load performance of the co-firing of coal and biomass in the power plant integrated with CCP and CCU is analysed in this study within a 40 to 100 % envelope in intervals of 20 %. Hence, part-load performance is estimated at 40, 60, 80 % of the base-load (100 %) power of the power plant for each co-firing case of coal and biomass. The methodology discussed by Hanak et al. (2015) is adopted for the boundary condition estimation at the part-load operation. The widely-followed control of the boilers are; the fixed pressure control for the boiler allowing steam throttling and the sliding pressure control for the boiler in which steam pressure follows the turbine load and is dictated by the boiler feed water pump. The sliding pressure control for the boiler is adopted as it results in reduced power consumption (Fernandez et al., 2016; Hanak et al., 2015). The heat transfer areas and temperature differences for the superheater, economiser reheater, and air preheater are kept constant as estimated by the direct-fired coal-based power plant case at base-load performance. Similarly, the heat transfer areas and temperature differences for the feedwater heaters are also kept constant, as estimated from the coal-fired power plant case at base-load. However, the pressure drop for the heat exchangers is estimated following the equation:

$$\Delta p = \frac{fV^2L}{2g\rho d} \tag{1}$$

Further, the pressure drops, which are based on homogenous flow conditions (Green, 2008) at the part-load performance, are updated using average velocity at base and part-load and pressure drops at base load, using the following equation (Hanak et al., 2015):

$$\Delta p_{part} = \frac{\left(\frac{V_{in_{part}} + V_{out_{part}}}{2}\right)^2}{\left(\frac{V_{in_{base}} + V_{out_{base}}}{2}\right)^2} \Delta p_{base} \tag{2}$$

The sliding pressure control of the boiler requires the estimation of the steam flowrates and pressure at different points of the steam turbine section along with the efficiencies for each turbine section. The constant temperature is maintained at each part-load performance from the 40 to 100 % load range by controlling the steam generation rate by the design specification rate (Hanak et al., 2015). The well-known equation, the Stadola Law of Cones (Cooke, 1983; Salisbury, 1950), is widely used in power plants for the off-design steam specifications estimation. The Stadola Law of Cones is used in an iterative manner for the fixed condenser pressure, and it is given as follows:

$$\frac{m_{in}}{m_{in_{base}}} = \frac{\mu\, p_{in}}{\mu_{base} p_{in_{base}}} \sqrt{\frac{p_{in_{base}} v_{in_{base}}}{p_{in} v_{in}}} \sqrt{\frac{1 - \left(\frac{p_{out}}{p_{in}}\right)^{\frac{n+1}{n}}}{1 - \left(\frac{p_{out_{base}}}{p_{in_{base}}}\right)^{\frac{n+1}{n}}}} \tag{3}$$

The isentropic efficiency is updated based on the base-load isentropic efficiencies of the turbine section. Knopf (2011) proposed the estimation of the isentropic efficiency based on the optimal design with 50 % of the reaction blading (a = 0.7071), for a constant shaft speed at different part-loads. Hence, the isentropic efficiency at the part-load can be estimated by the following equation (Knopf, 2011; Salisbury, 1950):

$$\frac{\eta_{part}}{\eta_{base}} \cong 2\,\frac{a}{\frac{v_{in_{base}}}{v_{in_{part}}}}\left[\left(a-\frac{a}{\frac{v_{in_{base}}}{v_{in_{part}}}}\right)+\sqrt{\left(a-\frac{a}{\frac{v_{in_{base}}}{v_{in_{part}}}}\right)^{2}+1-a^{2}}\right] \qquad (4)$$

At each part-load operation from 40 to 100 %, the effect of the integration of the CCP and CCU is also investigated. The CCP at the part-load performance of the power plant is kept to be the same size as reported in Table 4, as it is common in engineering practice to employ oversize units for better performance (Jordal et al., 2012). Therefore, the $CO_2$ capture rate is fixed at 90 % for part-load performance with 0.2 lean loading of the MEA 30 wt. % aqueous solution. At reduced flowrates, the CCU operation may be effected due to the flowrates approaching surge conditions. It is understood that anti surge control option is available for the CCU.

# 3 Results and discussion

## 3.1 Base-Load Performance

The reference coal-fired power plant integrated with CCP and CCU model is developed based on information provided in Sections 2.1 to 2.3 and Ali et al. (2017). Further, co-firing of coal and biomass for the CHI and CFF cases is evaluated for integration with CCP and CCU. The key performance results for supercritical co-firing coal and biomass power plants integrated with CCP and CCU for CHI case are reported in Table 5 for the base-load performance. The important results for co-firing coal and biomass in the pulverised supercritical power plants integrated with CCP and CCU for CFF case are reported in Table 6 for the base-load performance. The process flow diagram of the base-load direct-firing coal case with process parameters is indicated in Figure A-1.

Table 5 Important results for co-firing of coal and biomass in the pulverised supercritical power plants integrated with CCP and CCU for CHI case at base-load performance.

| Fuel type | Coal | C8B2 | C6B4 | C4B6 | C2B8 | Biomass |
|---|---|---|---|---|---|---|

| | | | | | | |
|---|---|---|---|---|---|---|
| Fuel [kg/s] | 71.3 | 75.6 | 80.4 | 85.9 | 92.3 | 99.6 |
| Total air [kg/s] | 729 | 726 | 723 | 720 | 712 | 702 |
| Slag + Fly Ash [kg/s] | 6.9 | 6 | 4.9 | 3.7 | 2.3 | 0.7 |
| Main steam [kg/s] | 630 | 630 | 630 | 630 | 630 | 630 |
| Reheat from boiler [kg/s] | 514 | 514 | 514 | 514 | 514 | 514 |
| Steam to stripper [kg/s] | 233 | 225 | 226 | 228 | 230 | 230 |
| Flue gas, absorber inlet [kg/s] | 832 | 830 | 829 | 827 | 819 | 804 |
| $CO_2$ composition in flue gas [mol%] | 13.28 | 13.42 | 13.56 | 13.73 | 13.93 | 14.35 |
| Lean MEA solution, absorber inlet [kg/s] | 2403 | 2414 | 2403 | 2453 | 2464 | 2470 |
| Specific reboiler duty [MJ/kg $CO_2$] | 3.686 | 3.679 | 3.677 | 3.675 | 3.674 | 3.673 |
| Total compression duty [$MW_e$] | 44.9 | 45.26 | 45.03 | 46.04 | 46.29 | 46.46 |
| Fuel heat input, HHV [$MW_{th}$] | 1933 | 1933 | 1933 | 1933 | 1933 | 1933 |
| Power without steam extraction [$MW_e$] | 800 | 800 | 800 | 800 | 800 | 800 |
| Power with steam extraction [$MW_e$] | 664 | 662 | 659 | 658 | 657 | 656 |
| Power without CCP and CCU [$MW_e$] | 758 | 758 | 758 | 758 | 758 | 758 |
| Power with CCP only [$MW_e$] | 602 | 600 | 598 | 597 | 596 | 596 |
| Power with CCP and CCU [$MW_e$] | 557 | 554 | 553 | 551 | 550 | 549 |
| Efficiency without CCP and CCU [%] | 39.22 | 39.3 | 39.3 | 39.3 | 39.3 | 39.3 |
| Efficiency with CCP only [%] | 31.16 | 31.02 | 30.94 | 30.86 | 30.83 | 30.82 |
| Efficiency with CCP and CCU [%] | 28.84 | 28.68 | 28.61 | 28.48 | 28.43 | 28.41 |

Table 6 Important results for co-firing of coal and biomass in the pulverised supercritical power plants integrated with CCP and CCU for CFF case at base-load performance.

| Fuel type | Coal | C8B2 | C6B4 | C4B6 | C2B8 | Biomass |
|---|---|---|---|---|---|---|
| Fuel [kg/s] | 71.3 | 71.3 | 71.3 | 71.3 | 71.3 | 71.3 |
| Total air [kg/s] | 729 | 685 | 641 | 598 | 550 | 502 |
| Slag + Fly Ash [kg/s] | 6.9 | 5.6 | 4.4 | 3.1 | 1.8 | 0.5 |

| | | | | | | |
|---|---|---|---|---|---|---|
| Main steam [kg/s] | 630 | 596 | 560 | 528 | 485 | 452 |
| Reheat from boiler [kg/s] | 514 | 486 | 457 | 431 | 396 | 369 |
| Steam to stripper [kg/s] | 233 | 212 | 198 | 188 | 176 | 163 |
| Flue gas, absorber inlet [kg/s] | 833 | 784 | 735 | 686 | 634 | 575 |
| $CO_2$ composition in flue gas [mol%] | 13.28 | 13.41 | 13.56 | 13.72 | 13.92 | 14.34 |
| Lean MEA solution, absorber inlet [kg/s] | 2403 | 2278 | 2128 | 2023 | 1889 | 1744 |
| Specific reboiler duty [MJ/kg $CO_2$] | 3.686 | 3.673 | 3.666 | 3.654 | 3.643 | 3.634 |
| Total compression duty [$MW_e$] | 44.9 | 42.8 | 40.06 | 38.22 | 35.82 | 33.21 |
| Fuel heat input, HHV [$MW_{th}$] | 1933 | 1823 | 1713 | 1603 | 1477 | 1384 |
| Power without steam extraction [$MW_e$] | 800 | 759 | 713 | 673 | 618 | 576 |
| Power with steam extraction [$MW_e$] | 664 | 627 | 590 | 555 | 509 | 475 |
| Power without CCP and CCU [$MW_e$] | 758 | 718 | 672 | 633 | 579 | 538 |
| Power with CCP only [$MW_e$] | 602 | 567 | 532 | 499 | 455 | 423 |
| Power with CCP and CCU [$MW_e$] | 557 | 524 | 492 | 461 | 419 | 390 |
| Efficiency without CCP and CCU [%] | 39.22 | 39.36 | 39.25 | 39.50 | 39.19 | 38.86 |
| Efficiency with CCP only [%] | 31.16 | 31.09 | 31.04 | 31.11 | 30.78 | 30.58 |
| Efficiency with CCP and CCU [%] | 28.84 | 28.75 | 28.70 | 28.72 | 28.36 | 28.18 |

The co-firing of coal and biomass results in more fuel feed requirement as the fraction of the biomass in the fuel stream increases for the CHI case and resulted in 40 % higher fuel flowrate for 100 % biomass in the fuel feed stream. However, the co-firing of coal and biomass causes considerable derating as the fraction of the biomass in the fuel stream increases for the CFF case and an overall 30 % derating of the power output capacity is expected for a complete switch to biomass compared to the reference coal power plant either integrated with CCP and CCU or not. The 44 and 49 % decrease in power output is expected when CCP and CCU, respectively, is integrated with the biomass fired plant compared with a standalone coal power plant.

However, the amount of the flue gas decreases and the $CO_2$ content in the flue gas increases, for the increased fraction of the biomass in the fuel due to the higher O/C ratio in the biomass for both the CHI and CFF cases. Also this results in higher specific $CO_2$ emissions from power plants when the biomass share in the fuel feed stream increases; resulting in more specific $CO_2$ capture from the power plant (Ali, 2017).

It is worth noting that the $CO_2$ composition in the flue gas and other process parameters of the direct-firing for the coal-fired and biomass-fired power plant are in good agreement with the values found in the literature (Al-Qayim et al., 2015; Hetland et al., 2016). Further, the amine-based CCP is extensively validated by the author in the literature (Akram et al., 2016; Ali et al., 2016). However, the literature lacks the data for the comparison of the process parameters with the reported values for the process validation and verification.

Moreover, if the biomass used is sustainably grown, it will result in more negative emissions from the system. Thus, results in a lower flow rate of the flue gas with higher concentration of the $CO_2$, hence lower solvent requirements for scrubbing, which decreases the specific reboiler duty. The effect of co-firing coal and biomass on the $CO_2$ composition in the flue and specific reboiler duty is given in Figure 2. However, there is a large decrease in specific reboiler duty for the CFF cases as compared to the CHI cases and this is due to the lower flue gas flowrates for the CFF cases and this results in the lower specific reboiler duty. The literature lacks sufficient data to verify or validate the CFF and CHI cases investigated in this study. However, the base cases of the coal-fired power plant was validated and verified by the author (Ali et al., 2017) and therefore the results of the CFF and CHI cases may be considered to be reliable.

The boiler model assumes an equilibrium approach, where the oxygen-rich environment will promote complete combustion. However, it is known that direct biomass combustion or co-combustion produces undesired pollutants, such as tar aerosols (e.g. polycyclic aromatic hydrocarbons (PAH)), soot, fine char particles and alkali-based aerosols (Williams et al., 2012). Experimental studies have shown that biomass (corn stalk and pine sawdust) addition for co-combustion decreases PAHs formation compared to coal combustion; particularly, 3-ring PAHs and higher rings are decreased for the blend cases (Zhou et al., 2016). Therefore, it is expected that for the presented co-firing cases, tar formation will decrease compared to coal combustion.

Co-firing of coal and biomass have substantial effect on the emission control technologies integrated with the power plant. As the sulphur content in the biomass is low, as reported in Table 1, the amount of by-product gypsum produced decreases with the increased share of biomass in the fuel feed stream. Hence, the FGD unit may not be required in the co-firing of coal and biomass at the higher biomass shares and the polisher unit may be enough to meet the $SO_2$ requirements at the absorber inlet of the CCP. In addition, the slag and fly ash decrease substantially when coal is replaced by biomass for both the CHI and CFF cases. The detailed key performance results for the different cases of the co-firing of the coal and biomass can be found in Tables A.1 and A.2 in the Appendix A for the CHI and CFF, respectively, for the base-load operation for more interpretation and explanation.

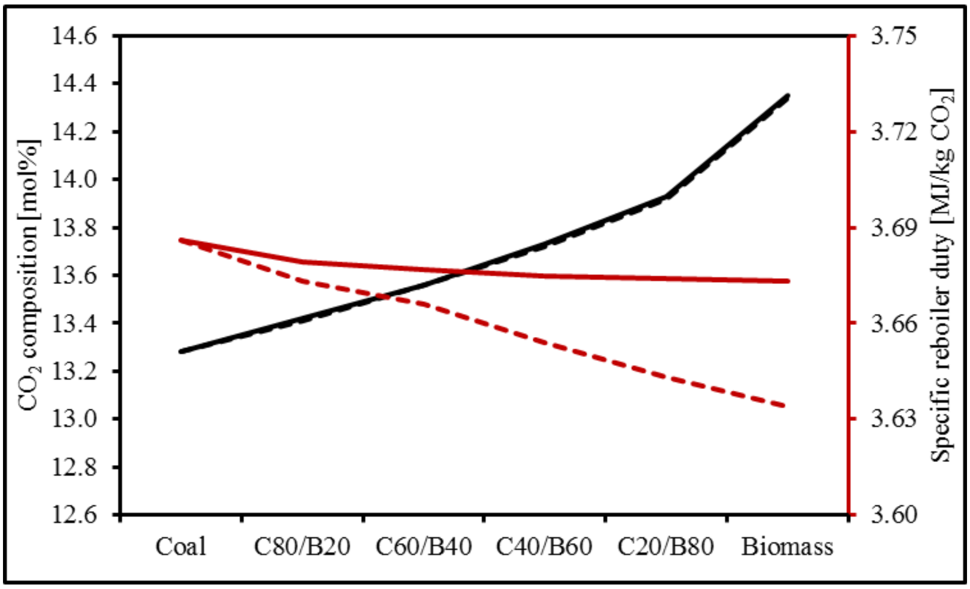


Figure 2 Impact of co-firing coal and biomass on the $CO_2$ composition in the flue gas and specific reboiler duty (where solid line represents CHI case and dashed line represents CFF case).

The net power output and net efficiency decreases when the share of biomass fraction in the fuel feed stream increases and this is due to a higher auxiliary load on the system for the CHI cases. It is observed that the efficiency penalty of the power plant with $CO_2$ capture and compression systems increases by approximately 4.8 % when coal is totally replaced by biomass in the CHI cases. However, there is a slight increase in specific $CO_2$ compression work per unit of the $CO_2$ captured and the specific losses per unit of the $CO_2$ captured due to increase in $CO_2$ concentration in the flue gas.

The efficiency penalty of the CFF cases is the same as that observed for the CHI cases since the base power output considered for comparison is the de-rated power output and not 800 $MW_e$. Due to the decreased flow rate of the flue gas, the amount of the $CO_2$ captured through scrubbing also decreases and hence results in a 30 % decrease in solvent requirement to scrub $CO_2$. Hence, this results in a considerable increase in the specific $CO_2$ compression work per unit of the $CO_2$ captured and specific losses per unit of the $CO_2$ captured for different CFF cases of co-firing of coal and biomass.

Table 7 Important results for co-firing of coal and biomass in the pulverised supercritical power plants integrated with CCP and CCU for the CFF case at 80, 60 and 40 % part-load performance.

| **Fuel type** | **Coal** | **C8B2** | **C6B4** | **C4B6** | **C2B8** | **Biomass** |
|---|---|---|---|---|---|---|
| | | | **80 % part-load operation** | | | |
| Fuel heat input, HHV [$MW_{th}$] | 1615 | 1523 | 1432 | 1340 | 1248 | 1156 |
| Power without steam extraction [$MW_e$] | 640 | 604 | 567 | 530 | 493 | 457 |
| Power with steam extraction [$MW_e$] | 523 | 488 | 452 | 423 | 393 | 365 |
| Power without CCP and CCU [$MW_e$] | 606 | 571 | 534 | 499 | 461 | 426 |
| Power with CCP only [$MW_e$] | 472 | 439 | 405 | 377 | 349 | 323 |
| Power with CCP and CCU [$MW_e$] | 435 | 403 | 371 | 345 | 319 | 295 |
| Efficiency without CCP and CCU [%] | 37.52 | 37.46 | 37.33 | 37.15 | 36.97 | 36.86 |
| Efficiency with CCP only [%] | 29.24 | 28.87 | 28.27 | 28.14 | 27.95 | 27.92 |
| Efficiency with CCP and CCU [%] | 26.91 | 26.47 | 25.90 | 25.76 | 25.55 | 25.52 |
| | | | **60 % part-load operation** | | | |
| Fuel heat input, HHV [$MW_{th}$] | 1262 | 1190 | 1118 | 1046 | 975 | 903 |
| Power without steam extraction [$MW_e$] | 480 | 452 | 425 | 398 | 370 | 343 |
| Power with steam extraction [$MW_e$] | 388 | 364 | 343 | 320 | 298 | 276 |
| Power without CCP and CCU [$MW_e$] | 454 | 427 | 400 | 374 | 346 | 320 |
| Power with CCP only [$MW_e$] | 349 | 326 | 307 | 296 | 264 | 244 |
| Power with CCP and CCU [$MW_e$] | 320 | 298 | 280 | 260 | 241 | 222 |
| Efficiency without CCP and CCU [%] | 35.98 | 35.85 | 35.79 | 35.72 | 35.50 | 35.40 |
| Efficiency with CCP only [%] | 27.66 | 27.42 | 27.43 | 27.24 | 27.1 | 26.99 |
| Efficiency with CCP and CCU [%] | 25.34 | 25.08 | 25.06 | 24.85 | 24.71 | 24.59 |
| | | | **40 % part-load operation** | | | |
| Fuel heat input, HHV [$MW_{th}$] | 882 | 832 | 781 | 731 | 681 | 631 |
| Power without steam extraction [$MW_e$] | 320 | 301 | 281 | 263 | 245 | 226 |
| Power with steam extraction [$MW_e$] | 268 | 252 | 235 | 220 | 204 | 189 |

| | | | | | | |
|---|---|---|---|---|---|---|
| Power without CCP and CCU [$MW_e$] | 303 | 284 | 264 | 247 | 229 | 210 |
| Power with CCP only [$MW_e$] | 241 | 226 | 210 | 196 | 181 | 167 |
| Power with CCP and CCU [$MW_e$] | 221 | 207 | 192 | 179 | 165 | 152 |
| Efficiency without CCP and CCU [%] | 34.30 | 34.12 | 33.84 | 33.73 | 33.61 | 33.32 |
| Efficiency with CCP only [%] | 27.37 | 27.20 | 26.91 | 26.82 | 26.58 | 26.48 |
| Efficiency with CCP and CCU [%] | 25.04 | 24.86 | 24.54 | 24.43 | 24.18 | 24.07 |

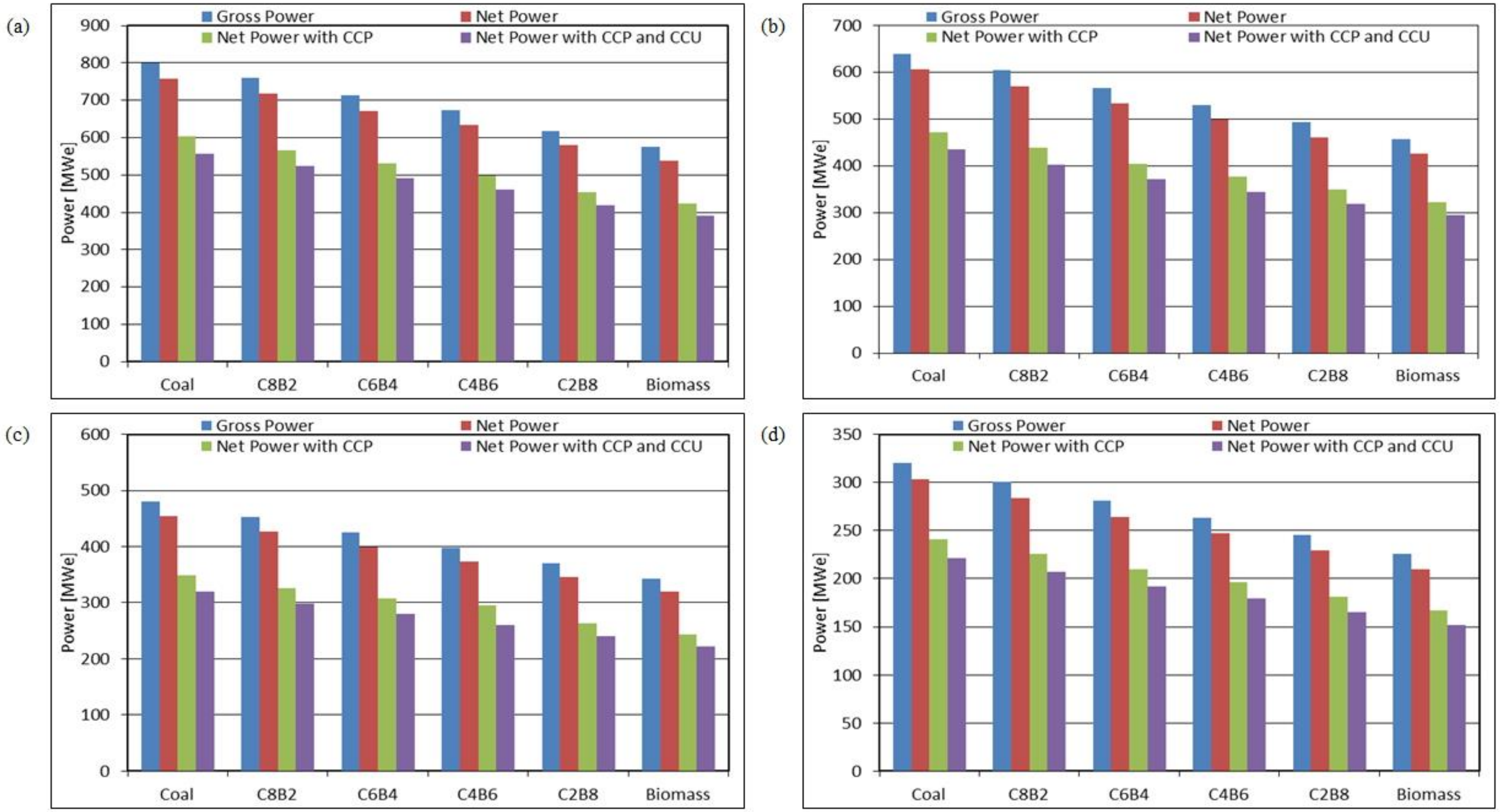


Figure 3 Power output from supercritical co-firing of coal and biomass power plants integrated with CCP and CCU for the CFF case at different part-load operations; (a) 100 % base-load operation; (b) 80 % part-load operation; (c) 60 % part-load operation; and (d) 40 % part-load operation.

### 3.2 Part-Load Performance

The part-load performance of the co-firing of coal and biomass integrated with CCP and CCU from 40 to 100 % load is evaluated for the CFF case. The operating conditions for the part-load operations were estimated based on the details provided in Section 2.3 for the referenced coal-fired power plant and then the co-firing of coal and biomass is assessed for integration with CCP and CCU for the CFF case for the part-load at 80, 60 and 40 % operation. Since, the case evaluated is CFF, the fuel flowrate for each of the part-load operation is kept constant at the same value as for the coal case at that part-load operation. Hence, this results in variable heat input and variable power output from the power plant with and without integration with CCP and CCU. However, co-firing of coal and biomass resulted in substantial power derating at each part-load operation. The power derating for different part-load operation integrated with CCP and CCU for the CFF case is shown in Figure 3 and listed in Table 7. The detailed performance results for part-load operation at 80, 60 and 40 % are given in Tables A.3, A.4 and A.5, respectively. The derating in power output efficiency of the power plant not only occurs horizontally when fuel is switched from coal to biomass at constant load operation, but it also degrades perpendicularly downward when the load is shifted to the lower ones for the same fuel type as listed in Table 3.

Furthermore, the behaviour of the power plant in terms of the power derating when fuel is switched from coal to biomass at constant part-load operation is similar, as clearly observed in Figure 3. An overall 30 to 32 % derating of the power output capacity is expected for complete switch to biomass compared to the reference coal power plant at each of the part-load operations either integrated with CCP and CCU or not. The 44 to 47 % and 49 to 51 % decrease in power output is expected when CCP and CCU, respectively, is integrated with the biomass fired plant compared with a standalone coal power plant at each part-load operation.

The specific reboiler duty behaviour is similar at each part-load operation as discussed in Section 3.1 for the base-load operation. However, for a specific ratio of coal and biomass co-firing, and subsequent part-load operation resulted in a decrease in specific reboiler duty, although this decrease is not linear in nature. The finding of the decrease of non-linearity is in line with the findings as found in the literature (Hanak et al., 2015). The decrease in specific reboiler duty is 0.74 % for load change from 80 % to 60 % and is 1.05 % for the load change from 60 % to 40 % of the part-load operation of the coal-fired power plant. Similarly, the decrease in specific reboiler duty is 0.71 % for a load change from 80 % to 60 % and 1.13 % for a load change from 60 % to 40 % of the part-load operation of the C8B2-fired power plant. Similarly, the by-products gypsum from FGD, fly-ash from ESP, slag from boiler and $NH_3$ requirement in SCR decreases not only with part-load operation for the specific fuel feed, but also for the co-firing at any of the part-load operation. It is important to mention here that an extensive study for the part-load operation of the co-firing of coal and biomass has not been found in the literature through which the results can be compared. However, since the base-case model was extensively validated and verified, and the results obtained are comparable then we have confidence in these results but this is a limitation of the present work.

As observed in the base-load operation, the flue gas treatment units may not be required when the biomass share in the fuel increases. A similar observation is found for the part-load co-firing of coal and biomass at different load operations. Process analysis revealed that the part-load operation of coal-fired power plant resulted in only 28 % of the total power (800$MW_e$) available on integration with CCP and CCU at 40 % load operation. The rest is degraded firstly due to load change and secondly due to the parasitic load of the CCP and CCU. Similarly, at part-load operation of the C8B2-fired power plant resulted in only 26 % of the total power (800$MW_e$) available on integration with CCP and CCU at 40 % load operation and 24 % for the C4B6 and eventually 19 % of the total power (800$MW_e$) available on integration with CCP and CCU at 40 % load operation for the biomass-fired power plant. Figure 4 shows the decrease in the power output due to the load change and further integration with CCP and CCU for different co-firing of coal and biomass at various load changes in the form of percentage of the total name plate power output of the power plant (800MW$_e$).

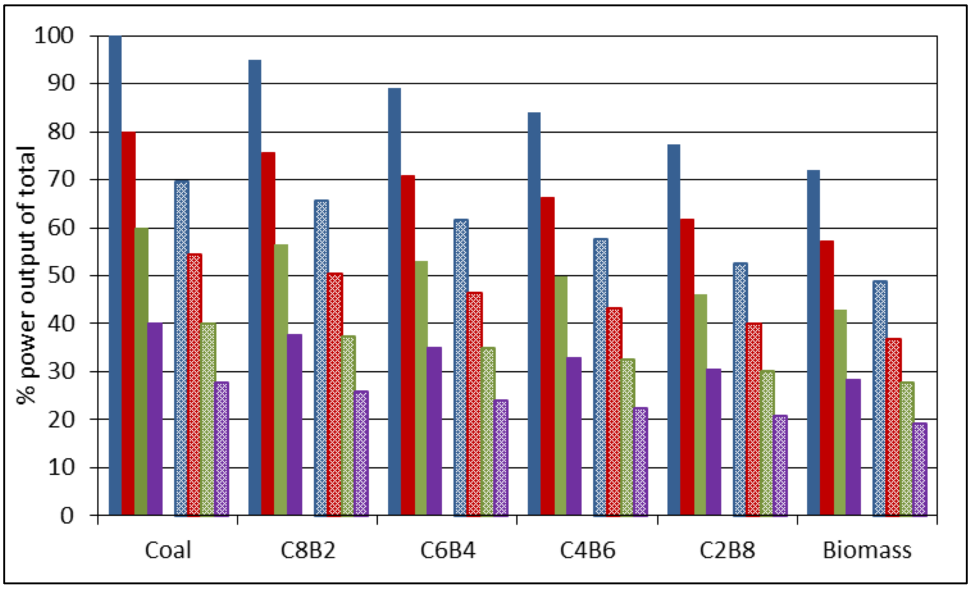


Figure 4 Percentage power output of the total name plate power output of the power plant (800MW$_e$) for integration with CCP and CCU for CFF case at different part-load operation where solid coloured bars are for % of the gross power output (of 800 MW$_e$) and hatched bars are for % of the net power output (of 800 MW$_e$) when integrated with CCP and CCU. Where blue: 100 % base-load operation; red: 80 % part-load operation; green: 60 % part-load operation; and purple: 40 % part-load operation.

The gross and net efficiency of direct-fired and co-fired coal and biomass power plants integrated with CCP and CCU for different part-load operations is shown in Figure 5. It is found that the gross efficiency and net efficiency of the power plants are reasonably constant on the fuel switch from direct coal-firing to co-firing coal and biomass and to direct biomass-firing. Since for the CFF case with co-firing the heat transfer decreases and hence the power produced varies and hence the ratio of the power and HHV remains almost constant. However, with the integration of the CCP and CCU there is a decrease in the efficiency as depicted as the net efficiency in Figure 5.

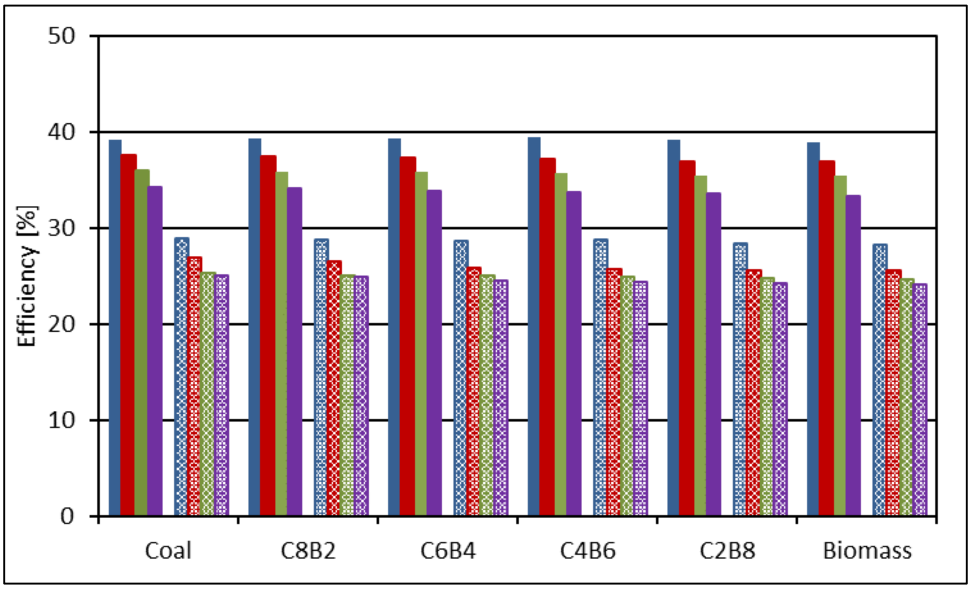


Figure 5 Efficiency for integration with CCP and CCU for CFF case at different part-load operation where solid coloured bars are for the gross efficiency and hatched bars are for the net efficiency when integrated with CCP and CCU. Where blue: 100 % base-load operation; red: 80 % part-load operation; green: 60 % part-load operation; and purple: 40 % part-load operation.

### 3.3 Effect of Part-Load on Operation of CCP

The net efficiency and power output of the power plant substantially reduces on integration with CCP and CCU at the part-load operation in reference to the standalone base power plant, and this will affect the operation and integration of the CCP (Hanak et al., 2015). Therefore, the steam demand and extraction form the cross-over of the IP-LP turbine will vary during the part-load operation. However, it is found that the power derating will not affect the operation of the CCP as with the power derating, the demand of the steam for $CO_2$ stripping decreases. Although, with power derating the IP-LP cross over pressure decreases and with a decrease in steam pressure the stripping equilibrium will be disturbed due to the reduced steam pressure and temperature (Fernandez et al., 2016). Furthermore, the amount of the $CO_2$ to be stripped out of the reduced volume flue gas decreases and is proportional to the load decrease in the power plant and results in less steam requirements (Fernandez et al., 2016). For example, at 40 % part-load operation, the steam temperature and pressure decreases to 254 $^{o}$C and 2.03 bar, respectively for biomass-fired power plant integrated with CCP and CCU. The capture rate of 90 % is still achievable through modelling as the amount of $CO_2$ to be stripped also reduces proportionally with the steam amount and the load changes.

However, it may not be possible to regenerate solvent at lower part-load operation when system non-idealities may also be taken into consideration. For these scenarios, interim solvent regeneration strategy may be adopted as suggested in the literature (Fernandez et al., 2016). Therefore, a more robust model of the CCP or dynamic studies needs to be performed for the evaluation of the CCP at part-load operation and this should be the subject for future research work.

# 4 Conclusions

This paper has investigated the part-load performance of a power plant for co-firing of coal and biomass in a commercial-scale pulverised supercritical power plant, integrated with an amine-based post-combustion $CO_2$ capture plant (CCP) and $CO_2$ compression unit (CCU). It is important to note that the results presented in this paper are for a specific composition of coal and biomass. However, these results can be generalised to other compositions as different co-firing scenarios are considered, and the predicted trends when increasing the biomass share will still be valid. However, the results and conclusions are case specific and depend on the composition of the coal and biomass selected. Furthermore, the model predictions of the direct-fired coal-based power plant are in very good agreement with the published data as reported by the author (Ali et al., 2017), and hence the results and findings of the present research may be used with confidence with a ± 10 % margin. Two co-firing scenarios of coal and biomass were investigated at base-load operation, and the following was concluded:

- At constant heat input (CHI), more fuel is required as the percentage of biomass is increased; e.g. for firing 100 % biomass, 40 % more fuel is fed than for 100 % coal.
- At constant fuel input (CFF), derating occurs as the fraction of the biomass in the fuel stream increases, e.g. 30 % derating of the power output capacity at firing 100 % biomass compared to 100 % coal.
- Higher specific $CO_2$ capture from the power plant is observed from when the share of biomass in the fuel feed increases due to increases in the $CO_2$ content in the flue gas, for both the CHI and CFF cases; it will result in negative emissions if sustainably-grown biomass is used.
- A larger decrease in specific reboiler duty is observed for the CFF cases as compared to the CHI cases and this is due to the lower flue gas flowrates.
- A FGD unit may not be required at the higher biomass shares, and a polisher unit may be enough to meet the $SO_2$ requirements at the absorber inlet due to the low sulphur content in biomass.
- The net power output and net efficiency decrease when the fraction of biomass increases for both cases. An efficiency penalty for integration with $CO_2$ capture and compression systems increases by approximately 4.8 % when firing 100 % biomass in the CHI case.

For part-load operation (80, 60 and 40 %) using the CFF case, the following was found:

- As expected, the power output decreases due to the load change and further integration with CCP and CCU for different levels of co-firing of coal and biomass. Co-firing of coal and biomass resulted in substantial power derating at each part-load operation. An overall 30 to 32 % derating of the power output capacity is expected for 100 % biomass.
- At each part-load operation, specific reboiler duty decreases when the biomass fraction increases.
- The by-products –gypsum from FGD, fly-ash from ESP, slag from boiler and $NH_3$ requirement in SCR– decrease for the co-firing at any part-load operation.

Future work will include the extension of the present work by including the various coal and biomass compositions in to consideration. Furthermore, comparing the cost and economics of the different systems under consideration.

## Nomenclature

### Abbreviations

| | |
|---|---|
| Abs | absorber |
| APH | air preheater |
| BECCS | bioenergy carbon capture and storage |
| CCP | $CO_2$ capture plant |
| CCS | carbon capture and storage |
| CCU | $CO_2$ compression unit |
| CFF | constant fuel flowrate |
| CHI | constant heat input |
| EM | economiser |

| | |
|---|---|
| ENRTL | electrolyte non-random two liquid |
| ESP | electro static precipitator |
| ETI | Energy Technology Institute |
| FGD | flue gas desulphurization |
| FWH | feedwater heater |
| GHG | greenhouse gases |
| HP | high pressure |
| IAPWS | International Association for the Properties of Water and Steam |
| ID | induced draft |
| IP | intermediate pressure |
| IPCC | Intergovernmental Panel on Climate Change |
| LP | low pressure |
| MEA | monoethanolamine |
| MPP3 | Maasvlakte power plant 3 |
| PAH | polycyclic aromatic hydrocarbons |
| RH | reheater |
| SCR | selective catalytic reduction |
| SH | superheater |
| TEG | tri ethylene glycol |
| WWC | water wash column |

**Parameters**

| | |
|---|---|
| $d$ | diameter (m) |
| $f$ | friction factor |
| $g$ | 9.8 $m/s^2$ |
| $L$ | length of section (m) |
| $m$ | mass flowrate (kg/s) |
| $p$ | pressure (bar) |
| $V$ | velocity (m/s) |
| $v$ | specific volume ($m^3/kg$) |
| $\eta$ | efficiency (%) |
| $\mu$ | kinematic viscosity ($m^2/s$) |
| $\rho$ | density ($kg/m^3$) |

**Subscripts**

| | |
|---|---|
| base | at base-load condition |
| in | input |
| part | at part-load condition |
| out | output |

# Acknowledgements

U Ali acknowledges the grant provided by the University of Engineering and Technology, Lahore Pakistan and the partial support by the University of Sheffield, UK for this research.

**References**

Adams, T., Mac Dowell, N., 2016. Off-design point modelling of a 420MW CCGT power plant integrated with an amine-based post-combustion $CO_2$ capture and compression process. Applied Energy 178, 681-702.
AG., S., 2014. Industrial Power: turbines for Biomass Plants – Products for Biomass-fired Power Generation and District Heating & Cooling Applications. Siemens AG., Energy Sector.
Agbonghae, E.O., Hughes, K.J., Ingham, D.B., Ma, L., Pourkashanian, M., 2014. Optimal Process Design of Commercial-Scale Amine-Based $CO_2$ Capture Plants. Industrial & Engineering Chemistry Research 53, 14815-14829.
Akram, M., Ali, U., Best, T., Blakey, S., Finney, K., Pourkashanian, M., 2016. Performance evaluation of PACT Pilot-plant for $CO_2$ capture from gas turbines with Exhaust Gas Recycle. International Journal of Greenhouse Gas Control 47, 137-150.
Al-Mansour, F., Zuwala, J., 2010. An evaluation of biomass co-firing in Europe. Biomass and Bioenergy 34, 620-629.
Al-Qayim, K., Nimmo, W., Pourkashanian, M., 2015. Comparative techno-economic assessment of biomass and coal with CCS technologies in a pulverized combustion power plant in the United Kingdom. International Journal of Greenhouse Gas Control 43, 82-92.
Ali, U., 2017. Process Simulation of Power Generation Systems with $CO_2$ Capture. PhD Thesis, University of Sheffield, Sheffield.
Ali, U., Agbonghae, E.O., Hughes, K.J., Ingham, D.B., Ma, L., Pourkashanian, M., 2016. Techno-Economic Process Design of a Commercial-Scale Amine-Based $CO_2$ Capture System for Natural Gas Combined Cycle Power Plant with Exhaust Gas Recirculation. Applied Thermal Engineering.
Ali, U., Font-Palma, C., Akram, M., Agbonghae, E.O., Ingham, D.B., Pourkashanian, M., 2017. Comparative potential of natural gas, coal and biomass fired power plant with post-combustion $CO_2$ capture and compression. International Journal of Greenhouse Gas Control 63, 184-193.
Alobaid, F., Karner, K., Belz, J., Epple, B., Kim, H.-G., 2014. Numerical and experimental study of a heat recovery steam generator during start-up procedure. Energy 64, 1057-1070.
Anderson, K., Bows, A., 2008. Reframing the climate change challenge in the light of post-2000 emission trends. Philosophical Transactions of the Royal Society 366, 3863-3883.
Azar, C., Lindgren, K., Mollersten, K., 2006. Carbon capture and storage from fossil fuels and biomass - costs and potential role in stabilizing the atmosphere. Climate Change 74, 47-49.
Azar, C., Lindgren, K., Obersteiner, M., Riahi, K., van Vuuren, D.P., den Elzen, K.M.G., Mollersten, K., Larson, E.D., 2010. The feasibility of low $CO_2$ concentration targets and the role of bioenergy with carbon capture and storage (BECCS). Climate change 100, 195-202.
Barbu, A., Dejean , F., Tomescu, M., Bottcher, H., Cludius, J., al., e., 2015, 4/2015. Trends and Projections in Europe 2015: Tracking Progress towards Europe's Climate and Energy Targets. European Environment Agency, Luxembourg.
Barbu, A., Schumacher, K., S, H., Hermann, H., Seimons, A., Zell, C., al., e., 2014, 6/2014. Trends and Projections in Europe 2014: Tracking Progress towards Europe's Climate and Energy Targets for 2020. European Environment Agency, Luxembourg.
BEIS, 2016. Renewable Heat Incentive (RHI) deployment data. Department for Business, Energy & Industrial Strategy.

Berstad, D., Arasto, A., Jordal, K., Haugen, G., 2011. Parametric study and benchmarking of NGCC, coal and biomass power cycles integrated with MEA-based post-combustion $CO_2$ capture. Energy Procedia 4, 1737-1744.
Bertrand, V., Dequiedt, B., Cadre, E.L., 2014. Biomass for electricity in the EU-27: Potential demand, $CO_2$ abatements and break even prices for co-firing. Energy Policy 73, 631-644.
Bhave, A., Taylor, R.S.H., Fennell, P., al., e., 2014. Screening and techno-economic assessment of biomass-based power generation with CCS technologies to meet 2050 $CO_2$ targets. Cambridge Centre for Computational Chemical Engineering, ISSN 1473-4273.
Biagini, E., Lippi, F., Petarca, L., Tognotti, L., 2002. Devolatilization rate of biomasses and coal biomass blends : an experimental investigation. Fuel 81, 1041-1050.
Biliyok, C., Lawal, A., Wang, M., Seibert, F., 2012. Dynamic modelling, validation and analysis of post-combustion chemical absorption $CO_2$ capture plant. International Journal of Greenhouse Gas Control 9, 428-445.
Black, J., 2010. Cost and performance baseline for fossil energy plants volume 1: bituminous coal and natural gas to electricity. Final report (2nd ed.) National Energy Technology Laboratory (2010 Nov) Report no.: DOE20101397.
Chou, V., Keairns, D., Turner, M., Woods, M., Zoelle, A., 2012. Quality guidelines for energy system studies: process modeling design parameters (National Energy Technology Laboratory) NETL. DOE-341/051314 pp 13–21.
Chou, V., Keairns, D., Turner, M., Woods, M., Zoelle, A., 2014. Quality guidelines for energy system studies: process modeling design parameters (National Energy Technology Laboratory) NETL. DOE-341/051314 pp 13–21.
EU Commission, 2006. Biomass Potential in Europe. European Commission (EC), Brussels, Belgium.
Cooke, D.H., 1983. Modeling of off-design multistage turbine pressures by Stodola's ellipse, Energy Incorporated PEPSE User's Group Meeting, Richmond, VA, Nov, pp. 2-3.
Cremers, M.F.G., 2009. Deliverable 4. Technical status of Biomass Co-Firing, 32. IEA Bioenergy Task Group.
Davidsson, K., Åmand, L.-E., Steenari, B.-M., Elled, A.-L., Eskilsson, D., Leckner, B., 2008. Countermeasures against alkali-related problems during combustion of biomass in a circulating fluidized bed boiler. Chemical Engineering Science 63, 5314-5329.
De, S., Assadi, M., 2009. Impact of cofiring biomass with coal in power plants–A techno-economic assessment. Biomass and Bioenergy 33, 283-293.
Dornburg, V., van Vuuren, D., van de Ven, G., Langeveld, H., Meeusen, M., Burger, N., al., e., 2010. Bioenergy revisited: Key factors in global potentials of bioenergy. Energy and Environmental Science 3, 258-267.
Driscoll, C.T., Buonocore, J.J., Levy, J.I., Lambert, K.F., Burtraw, D., Reid, S.B., Fakhraei, H., Schwartz, J., 2015. US power plant carbon standards and clean air and health co-benefits. Nature Climate Change 5, 535-540.
Ellis, N., Masnadi, M.S., Roberts, D.G., Kochanek, M.A., Ilyushechkin, A.Y., 2015. Mineral matter interactions during co-pyrolysis of coal and biomass and their impact on intrinsic char co-gasification reactivity. Chemical Engineering Journal 279, 402-408.
ETI, 2016. The evidence for deploying Bioenergy with CCS (BECCS) in the UK, An insights report from the Energy Technologies Institute. Energy Technologies Institute, Loughborough.
Fernandez, E.S., del Rio, M.S., Chalmers, H., Khakharia, P., Goetheer, E., Gibbins, J., Lucquiaud, M., 2016. Operational flexibility options in power plants with integrated post-combustion capture. International Journal of Greenhouse Gas Control 48, 275-289.
Gasser, T., Guivarch, C., Tachiiri, K., Jones, C., Ciais, P., 2015. Negative emissions physically needed to keep global warming below 2 °C. Nature Communications 6:7958, 1-7.
GCCSI, 2011. Global Status of BECCS Projects 2010. Global CCS Institute, Canberra, Australia.
GCCSI, 2015. Large Scale CCS Projects. the Global CCS Institute Database available on http://www.globalccsinstitute.com/projects/large-scale-ccs-projects. Assesed in January 2017.

GCCSI, 2016. The Global Status of CCS: 2016. Summary Report. Global CCS Institute, Canberra, Australia.

Gough, C., Upham, P., 2011. Biomass energy with carbon capture and storage (BECCS or Bio-CCS). Greenhouse Gases: Science and Technology 1, 324-334.

Green, D.W., 2008. Perry's chemical engineers' handbook, 8 ed. McGraw-hill New York.

Habibi, R., Kopyscinski, J., Masnadi, M.S., Lam, J., Grace, J.R., Mims, C.A., Hill, J.M., 2012. Co-gasification of biomass and non-biomass feedstocks: synergistic and inhibition effects of switchgrass mixed with sub-bituminous coal and fluid coke during $CO_2$ gasification. Energy & Fuels 27, 494-500.

Hanak, D.P., Biliyok, C., Manovic, V., 2015. Evaluation and modeling of part-load performance of coal-fired power plant with postcombustion $CO_2$ capture. Energy & Fuels 29, 3833-3844.

Heller, M.C., Keoleian, G.A., Msnn, M.K., Volk, T.A., 2004. Life cycle energy and environmental benefits of generating electricity from willow biomass. Renewable Energy 29, 1023-1042.

Hetland, J., Yowargana, P., Leduc, S., Kraxner, F., 2016. Carbon-negative emissions: Systemic impacts of biomass conversion: A case study on $CO_2$ capture and storage options. International Journal of Greenhouse Gas Control 49, 330-342.

Hughes, E.E., Tillman, D.A., 1998. Biomass cofiring: status and prospects 1996. Fuel processing technology 54, 127-142.

IEA, January 2007. Energy Technology Essentials, ETE03. International Energy Agency, Paris, France.

IPCC, 2014. Climate Change 2014: Mitigation of Climate Change. Intergovernmental Panel on Climate Change.

Jia, L., Geddis, P., Madrali, S., Preto, F., 2016. Determination of Emission Factors for Co-firing Biomass and Coal in a Suspension Fired Research Furnace. Energy and Fuels 30, 7342-7356.

Jordal, K., Ystad, P.A.M., Anantharaman, R., Chikukwa, A., Bolland, O., 2012. Design-point and part-load considerations for natural gas combined cycle plants with post combustion capture. International Journal of Greenhouse Gas Control 11, 271-282.

Klein, D., Bauer, N., Bodirsky, B., Dietrich, J.P., Popp, A., 2011. Bio-IGCC with CCS as a long-term mitigation option in a coupled energy-system and land-use model. Energy Proceedia 4, 2933-2940.

Knopf, F.C., 2011. Modeling, analysis and optimization of process and energy systems. John Wiley & Sons.

Koornneef, J., van Breevoort, P., Hamelinck, C., Hendriks, C., Hoogwijk, M., Koop, K., Koper, M., Dixnob, T., Camps, A., 2012. Global potential for biomass and carbon dioxide capture, transport and storage up to 2050. International Journal of Greenhouse Gas Control 11, 117-132.

Ledda, C., Schievano, A., Scaglia, B., Rossoni, M., Acién Fernández, F.G., Adani, F., 2016. Integration of microalgae production with anaerobic digestion of dairy cattle manure: an overall mass and energy balance of the process. Journal of Cleaner Production 112, Part 1, 103-112.

Loo, S.V., Koppejan, J., 2002. Handbook of biomass combustion and co-firing. Twente University Press, Enschede, the Netherlands.

Luckow, P., Wise, M.A., Dooley, J.J., Kim, S.H., 2010. Large-scale utilization of biomass energy and carbon dioxide capture and storage in the transport and electricity sectors under stringent $CO_2$ concentration limit scenarios. International Journal of Greenhouse Gas Control 4, 865-877.

Mann, M., Spath, P., 2001. A life cycle assessment of biomass cofiring in a coal-fired power plant. Clean Products and Processes 3, 81-91.

Masnadi, M.S., Grace, J.R., Bi, X.T., Ellis, N., Lim, C.J., Butler, J.W., 2015a. Biomass/coal steam co-gasification integrated with in-situ $CO_2$ capture. Energy 83, 326-336.

Masnadi, M.S., Grace, J.R., Bi, X.T., Lim, C.J., Ellis, N., 2015b. From fossil fuels towards renewables: Inhibitory and catalytic effects on carbon thermochemical conversion during co-gasification of biomass with fossil fuels. Applied Energy 140, 196-209.

Masnadi, M.S., Grace, J.R., Bi, X.T., Lim, C.J., Ellis, N., Li, Y.H., Watkinson, A.P., 2015c. From coal towards renewables: Catalytic/synergistic effects during steam co-gasification of switchgrass and coal in a pilot-scale bubbling fluidized bed. Renewable Energy 83, 918-930.

Möller, B.F., Genrup, M., Assadi, M., 2007. On the off-design of a natural gas-fired combined cycle with $CO_2$ capture. Energy 32, 353-359.
Muratori, M., Calvin, K., Wise, M., Kyle, P., Edmonds, J., 2016. Global economic consequences of deploying bioenergy with carbon capture and storage (BECCS), Environmental Research Letters, pp. 1-9.
NETBIOCOF, 2016. D14: First state-of-the-art report. Integrated European Network for Biomass Co-firing (NETBIOCOF).
Nord, L.O., Anantharaman, R., Bolland, O., 2009. Design and off-design analyses of a pre-combustion $CO_2$ capture process in a natural gas combined cycle power plant. International Journal of Greenhouse Gas Control 3, 385-392.
Oladejo, J.M., Adegbite, S., Pang, C.H., Liu, H., Parvez, A.M., Wu, T., 2017. A novel index for the study of synergistic effects during the co-processing of coal and biomass. Applied Energy 188, 215-225.
Ortiz, D.S., Curtright, A.E., Samaras, C., Litovitz, A., Burger, N., 2011. Near-Term Opportunities for Integrating Biomass into the U.S. Electricity Supply. RAND Corporation.
Oxburgh, R., 2016. Lowest Cost Decarbonisation for the UK: The Critical Role of CCS. Report to the Secretary of State for Business, Energy and Industrial Strategy from the Parliamentary Advisory Group on Carbon Capture and Storage (CCS).
Rigamonti, L., Grosso, M., Biganzoli, L., 2012. Environmental assessment of refuse-derived fuel co-combustion in a coal-fired power plant. Journal of Industrial Ecology 16, 748-760.
Sahu, S.G., Chakraborty, N., Sarkar, P., 2014. Coal–biomass co-combustion:Anoverview. Rnewable and Sustainable Energy Reviews 39, 575-586.
Salisbury, J.K., 1950. Steam turbines and their cycles. Wiley.
Sebastián, F., Royo, J., Gómez, M., 2011. Cofiring versus biomass-fired power plants: GHG (Greenhouse Gases) emissions savings comparison by means of LCA (Life Cycle Assessment) methodology. Energy 36, 2029-2037.
Stultz, S., Kitto, J., 1992. Steam, Its Generation and Use, 1st Print. Babcock & Wilcox, AD.
Sung, Y., Lee, S., Kim, C., Jun, D., Moon, C., Choi, G., Kim, D., 2016. Synergistic effect of co-firing woody biomass with coal on NOx reduction and burnout during air-staged combustion. Experimental Thermal and Fluid Science 71, 114-125.
Thompson, T.M., Rausch, S., Saari, R.K., Selin, N.E., 2014. A systems approach to evaluating the air quality co-benefits of US carbon policies. Nature Climate Change 4, 917-923.
Tilghman, M.B., Mitchell, R.E., 2015. Coal and biomass char reactivities in gasification and combustion environments. Combustion and Flame 162, 3220-3235.
Tillman, D.A., 2000. Biomass cofiring: the technology, the experience, the combustion consequences. Biomass and Bioenergy 19, 365-384.
Toshiba, 2016. Toshiba and Mizuho Information & Research Institute to Lead Japan's Largest CCS Project. Press release available from: https://www.toshiba.co.jp/about/press/2016_07/pr2601.htm. Assesed in January 2017.
Verhoest, C., Ryckmans, Y., June 2014. Industrial Wood Pellets: Report Pellcert. Laborelec.
Wang, C., Wang, F., Yang, Q., Liang, R., 2009. Thermogravimetric studies of the behaviour of wheat straw with added coal during combustion. Biomass and Bioenergy 33, 50-56.
West , J., Smith, S.J., Silva, R.A., Naik, V., Zhang, Y., Adelman, Z., Fry, M.M., Anenberg, S., Horowitz, L.W., Lamarque, J.F., 2013. Co-benefits of mitigating global greenhouse gas emissions for future air quality and human health. Nature Climate Change 3, 885-889.
Williams, A., Jones, J., Ma, L., Pourkashanian, M., 2012. Pollutants from the combustion of solid biomass fuels. Progress in Energy and Combustion Science 38, 113-137.
Zhou, C., Liu, G., Wang, X., Qi, C., 2016. Co-combustion of bituminous coal and biomass fuel blends: Thermochemical characterization, potential utilization and environmental advantage. Bioresource technology 218, 418-427.